PERSPECTIVE

OBC
www.rsc.org/obc

New perspective of electron transfer chemistry

Shunichi Fukuzumi
Department of Material and Life Science, Graduate School of Engineering, Osaka University, CREST, Japan Science and Technology Corporation (JST), 2-1 Yamada-oka, Suita, Osaka 565-0871, Japan

Received 3rd January 2003
First published as an Advance Article on the web 30th January 2003

A new perspective of electron transfer chemistry is described for fine control of electron transfer reactions including back electron transfer in the charge separated state of artificial photosynthetic compounds and its synthetic application. Fundamental electron transfer properties of suitable components of efficient electron transfer systems are described in light of the Marcus theory of electron transfer, in particular focusing on the Marcus inverted region, and they are applied to design multi-step electron transfer systems which can well mimic the function of a photosynthetic reaction center. Both intermolecular and intramolecular electron transfer processes are finely controlled by complexation of radical anions, produced in the electron transfer, with metal ions which act as Lewis acids. Quantitative measures to determine the Lewis acidity of a variety of metal ions are given in relation to the promoting effects of metal ions on the electron transfer reactions. The mechanistic viability of metal ion catalysis in electron transfer reactions is demonstrated by a variety of examples of chemical transformations involving metal ion-promoted electron transfer processes as the rate-determining steps, which are made possible by complexation of radical anions with metal ions.

1 Introduction

Electron transfer is one of the most fundamental chemical reactions, playing a pivotal role not only in chemical processes but also in biological redox processes, which are essential for life, such as photosynthesis and respiration, since an electron is the minimal unit of the change in chemical reactions. During the past half-century, the field of electron transfer chemistry has undergone a remarkable expansion by the detailed analytic theory developed by R. A. Marcus[1] and also by the introduction of new technology such as lasers which have expanded the electron transfer systems which could be studied, extending it to ultra fast reactions in even the femtosecond regime.[2] The most important prediction of the Marcus theory of electron transfer is that the electron transfer rate is expected to decrease rather than to increase as the driving force of electron transfer ($-\Delta G^0_{et}$) increases in the region where the driving force is larger than the reorganization energy of electron transfer ($-\Delta G^0_{et} > \lambda$).[1] The reorganization energy of electron transfer (λ) is the energy required to structurally reorganize the donor, acceptor and their solvation spheres upon electron transfer. When the free energy change of electron transfer (ΔG^0_{et}) becomes very negative, the driving force of electron transfer ($-\Delta G^0_{et}$) can exceed the reorganization energy (λ). This region ($-\Delta G^0_{et} > \lambda$) is generally referred to as the Marcus inverted region. In the normal region ($-\Delta G^0_{et} < \lambda$), the electron transfer rate increases with increasing driving force, namely increasingly negative ΔG^0_{et}, but in the Marcus inverted region the opposite is true. In the beginning, the Marcus inverted region was tested for intermolecular electron transfer reactions of electron donors and electron acceptors at diffusional encounter. However, definitive evidence for the inverted region had been almost nonexistent for a long time.[3–6] Normally, these intermolecular electron transfer reactions follow the Rehm–Weller behavior such that the electron transfer rate increases with an increase in driving force, reaches a diffusion-limit and remains unchanged no matter how exergonic the electron transfer might become.[7–9] This is the reason why some twenty-five years elapsed before the existence of the Marcus inverted region was confirmed experimentally in the back electron transfer process (first-order decay) in the radical ion pair produced by intermolecular electron transfer reactions,[10] and also in a number of systems with donor–acceptor, where covalent linkages ensure fixed distances.[11–15] Intermolecular electron transfer systems at diffusional encounter (bimolecular second-order processes) exhibiting the Marcus inverted behavior have still remained largely unexplored as compared with the unimolecular first-order electron transfer processes.

Rates of electron transfer reactions of a variety of electron donor–acceptor systems can be well predicted in light of the Marcus theory of electron transfer, once the fundamental electron transfer properties of electron donors and acceptors such as the one-electron redox potentials and the reorganization energies of electron transfer are determined.[16] In other words, the electron transfer systems can now be well-designed based on the fundamental electron transfer properties of reactant molecules. However, design of electron transfer systems has so far been limited mainly to two-component systems, *i.e.*, electron donor–acceptor systems. In contrast, introduction of an appropriate third component acting as an effective catalyst has been a central issue in designing modern chemical reactions which involve cleavage and formation of chemical bonds.

On the other hand, the catalytic control of electron transfer systems has yet to emerge as an identifiable field of study, although a variety of metal enzymes are involved in controlling electron transfer processes in biological redox systems.[17] The conceptual lack of catalysis in electron transfer reactions stems from the general belief that there may be no need of catalysis to accelerate further an electron transfer reaction which is already fast enough in a practical sense. This is largely true for reversible electron transfer reactions in which electron transfer occurs only when the free energy change of electron transfer is negative, *i.e.*, the electron transfer is exergonic ($\Delta G^0_{et} < 0$). If the electron transfer is endergonic ($\Delta G^0_{et} > 0$), no net electron transfer would occur because of facile back electron transfer to regenerate the reactant pair. However, numerous chemical reactions, previously formulated by "movements of electron pairs" are now understood as processes in which an initial electron transfer from a nucleophile (reductant) to an electrophile (oxidant) produces a radical ion pair, which leads to the final products *via* the follow-up steps involving cleavage and formation of chemical bonds.[18–20] The follow-up steps are usually sufficiently rapid to render the initial electron transfer the rate-determining step in an overall irreversible chemical transformation. In such a case, promotion of the rate-determining electron transfer step, which is usually endergonic ($\Delta G^0_{et} > 0$) and thereby thermodynamically unfavorable, would play an essential role in accelerating the overall chemical reaction. Since electron transfer is an elementary reaction, acceleration of the rate of electron transfer with a "promoter" should involve change in

DOI: 10.1039/b300053b

the driving force of electron transfer by binding of the promoter to a product of the electron transfer.[21] However, a promoter becomes equivalent to a catalyst when the promoted initial electron transfer is the rate-determining step in an overall irreversible chemical transformation and the promoter is not involved in the final products.[21]

This article is intended to focus on recent advancement in understanding and insight gained in the fundamental studies of electron transfer systems particularly focusing on the Marcus inverted region[1] and also on the catalytic control of intermolecular and intramolecular electron transfer processes. First, fundamental electron transfer properties of suitable components of efficient electron transfer systems are described in light of the Marcus theory of electron transfer and they are applied to construct multi-step electron transfer systems which can well mimic the function of a photosynthetic reaction center. Then, it is shown that introduction of a third component acting as a promoter in electron transfer reactions provides a new perspective of electron transfer chemistry, expanding the scope of electron transfer systems which would otherwise be impossible to study.[19–21] The mechanistic viability of catalytic control of electron transfer reactions is demonstrated by a variety of examples of chemical transformations involving electron transfer processes as the rate-determining step, which are made possible by the introduction of an appropriate promoter.

2 Suitable components of efficient electron transfer systems

Porphyrins contain an extensively conjugated two-dimensional π system, which is suitable for efficient electron transfer, because the uptake or release of electrons results in minimal structural change upon electron transfer.[22] Porphyrin π radical cations are known to play a crucial role in biological electron transfer systems such as respiration and photosynthesis.[22] Efficient electron transfer between a porphyrin and the corresponding π radical cation is shown by the EPR linewidth variation of the EPR spectra of zinc porphyrin radical cations in the presence of the neutral form.[23] The linewidth of the EPR signal of $ZnP^{\bullet+}$ [P^{2-} = 5,10,15,20-tetrakis(3,5-di-*tert*-butylphenyl)porphyrin dianion] becomes broader as the temperature is decreased from 313 K to 233 K.[23] This indicates that the electron self-exchange reaction becomes faster at a lower temperature. The rate constants (k_{ex}) of the electron self-exchange reactions between $ZnP^{\bullet+}$ and ZnP were determined from an increase in the linewidth with increasing ZnP concentration. The activation parameters are determined from the Arrhenius plots in Fig. 1, where the positive slopes for the data in toluene, CH_2Cl_2 and $CHCl_3$ afford the negative activation enthalpies ($\Delta H^{\neq}_{obs} < 0$).[23] In acetonitrile (MeCN), however, a normal negative slope is obtained to afford the positive $\Delta H^{\neq}_{obs}$ value. The negative activation enthalpy indicates that the electron self-exchange reaction proceeds *via* a charge transfer π complex formed between $ZnP^{\bullet+}$ and ZnP, and that the activation energy of electron transfer in the π complex is smaller than the stabilization energy of the π complex (Scheme 1).[23] In the electron self-exchange reaction, there is no net change in solvation before

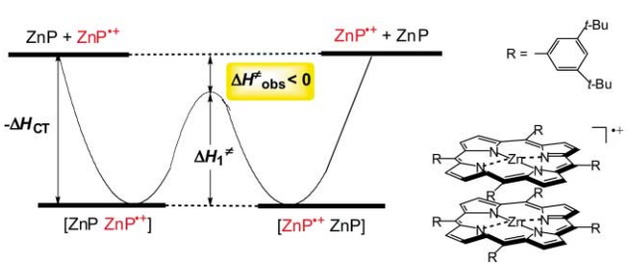

Scheme 1 Energy diagram of the electron exchange reactions between $ZnP^{\bullet+}$ and ZnP.[23]

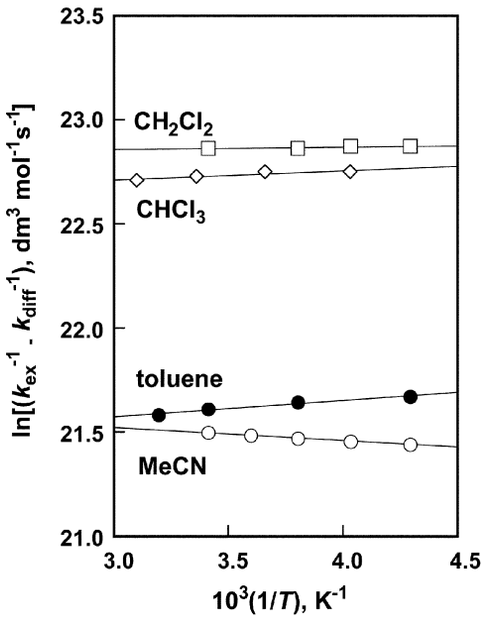

Fig. 1 Arrhenius plots of the electron self-exchange reaction between $ZnP^{\bullet+}$ and ZnP in different solvents.[23]

and after the electron transfer, when the solvent reorganization energy of electron transfer becomes smaller as the solvent polarity decreases.[24] This may be the reason why a negative activation enthalpy is observed for the $ZnP^{\bullet+}$/P system in less polar solvents such as CH_2Cl_2, $CHCl_3$ and toluene as compared to the case in MeCN (Fig. 1).

A sandwich-like structure for the dimeric aromatic π radical cations has been well-established.[25,26] The X-ray structure and the intervalent electron transfer in organic mixed-valence crystals with bridged aromatic radical cations are also reported.[27]

In contrast with the two-dimensional porphyrin π-system, fullerenes contain an extensively conjugated three-dimensional π system. Buckminsterfullerene (C_{60}), for example, is described as having a closed-shell configuration consisting of 30 bonding molecular orbitals with 60 π-electrons,[28] which is also suitable for efficient electron transfer. In fact, C_{60} is an ideal molecule to examine the electron transfer reactions in light of the Marcus electron transfer theory, since C_{60} is essentially spherical. The first electron in the reduction of C_{60} is added to a triply degenerate t_{1u} unoccupied molecular orbital and is highly delocalized.[29] Thus, electron transfer to C_{60} is expected to be highly efficient because of the minimal changes of structure and solvation associated with the electron transfer reduction. The efficiency of electron transfer is demonstrated by the electron self-exchange rate between C_{60} and the radical anion ($C_{60}^{\bullet-}$). Since C_{60} contains no protons which exhibit hyperfine splitting in the EPR spectrum, a *t*-butyl radical is attached on C_{60} to examine the electron self-exchange reaction between *t*-$BuC_{60}^{\bullet}$ and *t*-BuC_{60}^{-} [eqn. (1)] by analyzing linewidth variations of the EPR spectra.[30]

(1)

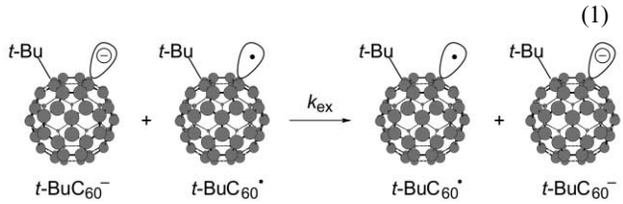

The rate constant (k_{ex}) of the electron self-exchange reaction between *t*-$BuC_{60}^{\bullet}$ and *t*-BuC_{60}^{-} was determined as 1.9×10^8 dm^3 mol^{-1} s^{-1} at 298 K.[30] This value corresponds to the reorganization energy (λ) of 0.64 eV. The observed λ value mainly consists of the solvent reorganization energy associated

with the electron transfer, since the bond reorganization of fullerenes in electron transfer has been evaluated to be negligibly small.[30,31]

The small reorganization energy of electron transfer of fullerenes has enabled observation of the Marcus inverted region in intermolecular electron transfer from fullerenes (C_{60}, C_{76} and C_{78}) to a series of arene radical cations produced by pulse-radiolysis in dichloromethane (CH_2Cl_2) [eqns. (2)–(4)].[32]

$$CH_2Cl_2 \longrightarrow CH_2Cl_2^{\bullet +} + e_s^- \qquad (2)$$

$$\text{arene} + CH_2Cl_2^{\bullet +} \longrightarrow \text{arene}^{\bullet +} + CH_2Cl_2 \qquad (3)$$

$$\text{fullerene} + \text{arene}^{\bullet +} \xrightarrow{k_{et}} \text{fullerene}^{\bullet +} + \text{arene} \qquad (4)$$

The one-electron oxidation potentials of the employed arenes—corresponding to the one-electron reduction potentials of arene π radical cations—were determined in CH_2Cl_2 to evaluate the driving forces of electron transfer oxidation of fullerenes with arene π-radical cations.[32] The driving force dependence of the logarithm of the rate constant of intermolecular electron transfer (log k_{et}) shows a pronounced decrease towards the highly exothermic region, representing the definitive confirmation of the existence of the Marcus inverted region in a truly intermolecular electron transfer (Fig. 2).[32] The plateau in Fig. 2 corresponds to the diffusion-limited region where the rate of electron transfer is faster than the rate of diffusion. According to the Marcus theory of electron transfer,[1] the observed rate constant of an adiabatic intermolecular electron transfer is given by eqn. (5),

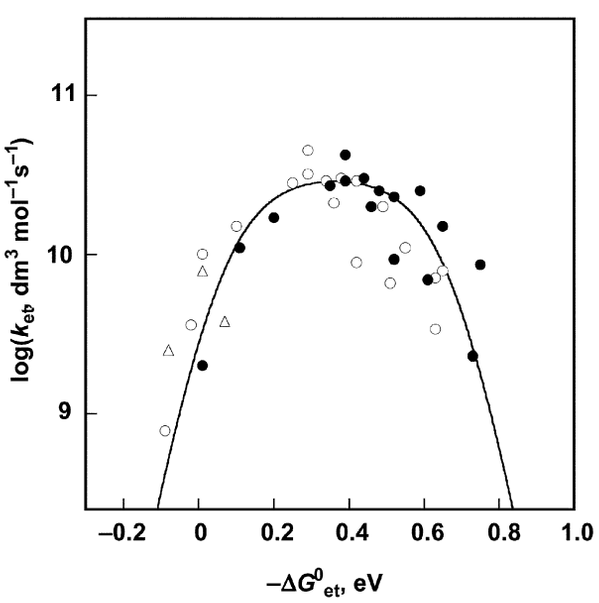

Fig. 2 Plot of log k_{et} *vs.* $-\Delta G^0_{et}$ for electron transfer from C_{60} (△), C_{76} (○) and C_{78} (●) to arene radical cations in CH_2Cl_2.[32] The solid line is drawn based on the Marcus theory of electron transfer [eqn. (5)].

$$\frac{1}{k_{et}} = \frac{1}{k_{diff}} + \frac{1}{Z \exp\left[-(\lambda/4)\left(1 + \Delta G^0_{et}/\lambda\right)^2 / k_B T\right]} \qquad (5)$$

where k_{diff} is the diffusion rate constant and k_B is the Boltzmann constant. By fitting the data in Fig. 2 with the Marcus equation for adiabatic bimolecular electron transfer reactions [eqn. (5)], the reorganization energy (λ) is determined as 0.36 eV for the electron transfer oxidation of fullerenes (C_{60}, C_{76} and C_{78}) in CH_2Cl_2.[32] This is the smallest value for bimolecular electron transfer reactions ever reported.

Electron transfer reduction of fullerenes with anthracene radical anions was also examined by laser flash photolysis in benzonitrile (PhCN).[32] A significant decrease in the k_{et} value was observed at large driving forces as compared to the diffusion-limited value seen at smaller driving forces as in the case of the electron transfer oxidation. The λ value for the electron transfer reduction of fullerenes is determined as 0.72 eV.[32] The larger λ value for the electron transfer reduction of C_{60} in PhCN than the λ value for the electron transfer oxidation of fullerenes in CH_2Cl_2 (0.36 eV) results from the larger solvent reorganization in the more polar solvent.

3 Long lifetimes of charge-separated states

The Marcus inverted region plays an essential role in photosynthesis, where a relay of electron transfer reactions evolves among chlorophyll- and quinone-moieties embedded in a transmembrane protein matrix.[33,34] Relatively little energy (0.2 eV) is consumed in the rapid initial photoinduced electron transfer step from bacteriochlorophyll dimer [$(BChl)_2$] to bacteriopheophytin (Bphe) on a time scale of 3 ps. In contrast, the back electron transfer to the ground state has nearly 1.2 eV of driving force, and thereby should be within the Marcus inverted region, where the rate of electron transfer decreases with increasing the driving force.[1] In such a case a charge shift reaction from $Bphe^{\bullet -}$ to an electron acceptor quinone (Q_A) occurs much faster on a time scale of 200 ps than the back electron transfer which occurs on a time scale of 10 ns. The system undergoes further charge separation, achieving a nearly quantitative quantum yield of the final charge-separated state which has an extremely long lifetime (*ca.* 1 s).

The mimicry of these complex and highly versatile processes has been achieved by using a suitable chromophore and a redox component, having small reorganization energies of electron transfer, namely porphyrins (or chlorines) and fullerenes, which are linked with covalent bonds.[35–38] The photoexcitation of zinc chlorin–C_{60} (ZnCh–C_{60}), free-base chlorin–C_{60} (H_2Ch–C_{60}), zinc porphyrin–C_{60} (ZnPor–C_{60}) and free-base porphyrin–C_{60} (H_2Por–C_{60}) dyads results in efficient electron transfer from the singlet excited states of the chromophore to C_{60}.[35,36] The driving force dependence of the rate constants (log k_{ET}) for the intramolecular photoinduced electron transfer for the charge separation (CS) process is shown in Fig. 3.[36] According to the Marcus theory of electron transfer,[1b] the rate constant of nonadiabatic intramolecular electron transfer (k_{ET}) is given by eqn. (6), where V is the electronic coupling matrix element, h is the Planck constant, and T is the absolute temperature.

$$k_{ET} = \left(\frac{4\pi^3}{h^2 \lambda\, k_B\, T}\right)^{1/2} V^2 \exp\left[-\frac{\left(\Delta G^0_{ET} + \lambda\right)^2}{4\lambda\, k_B\, T}\right] \qquad (6)$$

By fitting the data of the CS process in Fig. 3 with eqn. (6), the λ and V values were determined as $\lambda = 0.48$ eV and $V = 6.8$ cm^{-1}, respectively.[36] The λ value (0.48 eV) for the intramolecular CS process is smaller than the value for intermolecular electron transfer reduction of C_{60} in PhCN (0.72 eV).[32] This may result from a short edge-to-edge distance (R_{ee}) of the present dyad system (5.89 Å),[35] since the smaller the R_{ee}, the smaller will be the solvent reorganization energy as expected from the Marcus theory of electron transfer.[1] The smaller R_{ee} value also results in the larger V value.

The photoinduced CS processes in the dyads are located in the normal region of the Marcus parabola ($-\Delta G^0_{et} > \lambda$) whereas the back electron transfer from $C_{60}^{\bullet -}$ to $ZnCh^{\bullet +}$ in the CS state [charge recombination (CR) process] is in the Marcus inverted region ($-\Delta G^0_{BET} < \lambda$). In the inverted region, the k_{BET} value is expected to decrease with increasing driving force.[1] In fact, the photoexcitation of ZnCh–C_{60} results in an unusually long-lived radical ion pair detected as the transient absorption spectrum of $ZnCh^{\bullet +}$–$C_{60}^{\bullet -}$ (λ_{max} = 1000 nm due to $C_{60}^{\bullet -}$ and

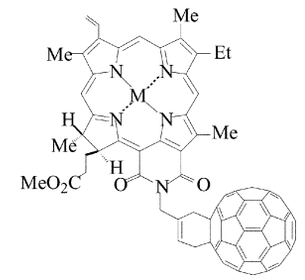

M = Zn (**1**, ZnCh–C_{60})
= H_2 (**3**, H_2Ch–C_{60})

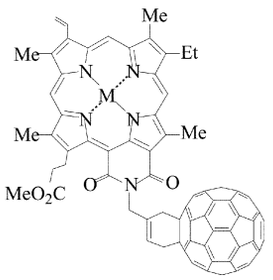

M = Zn (**2**, ZnPor–C_{60})
= H_2 (**4**, H_2Por–C_{60})

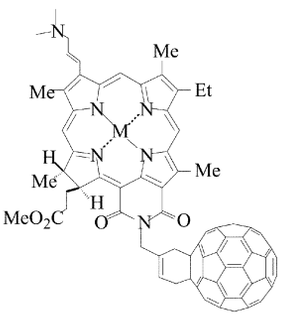

M = Zn (**5**, ZnCh–C_{60})

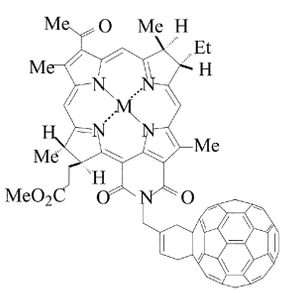

M = H_2 (**6**, H_2BCh–C_{60})

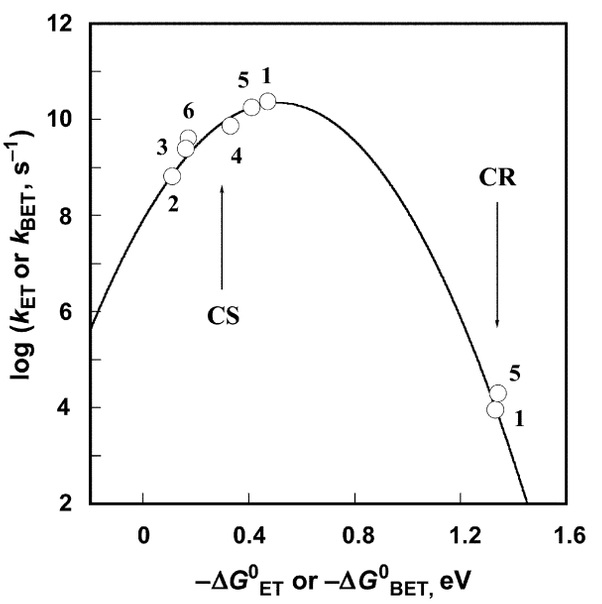

Fig. 3 Plot of log k_{ET} *vs.* $-\Delta G^0_{ET}$ for photoinduced charge separation (CS) of zinc chlorin-C_{60}, free-base chlorin-C_{60}, zinc porphyrin-C_{60} and free-base porphyrin-C_{60} dyads and log k_{BET} *vs.* $-\Delta G^0_{BET}$ back electron transfer [charge recombination (CR)] in the CS states. The data were taken from ref. 35. The solid line is drawn based on the Marcus theory of intramolecular electron transfer [eqn. (6)].

790 nm due to $ZnCh^{\bullet+}$) which decays *via* first-order kinetics with a decay rate constant of 9.1×10^3 s^{-1} (lifetime: 110 μs).[35] This value is also well fitted by the Marcus equation [eqn. (5)] with the same λ and V values (Fig. 3).

In contrast to the case of ZnCh–C_{60}, no transient formation of $C_{60}^{\bullet-}$ was detected at 1000 nm for any other dyad, H_2Ch–C_{60}, ZnPor–C_{60} or H_2Por–C_{60}.[35] In each case, only the triplet–triplet absorption due to the chlorin or porphyrin moiety was observed due to the higher energy of the radical ion pair as compared to the triplet excited state.[36] The E^0_{red} values for reduction of linked C_{60} which are attributed to the fullerene moiety are almost invariant irrespective of the type of linked macrocyclic ring whereas the E^0_{ox} values for oxidation of the macrocycle are shifted in a negative direction in the following order: H_2Por > H_2Ch > ZnPor > ZnCh.[35] Thus, the free energy change of electron transfer from ZnCh to C_{60}, obtained from the difference between E^0_{ox} and E^0_{red}, is the smallest among the examined dyads. In this case, the radical ion pair state ($ZnCh^{\bullet+}$–$C_{60}^{\bullet-}$) is lower in energy (1.33 eV) than both the triplet excited state of C_{60} (1.45 eV) and ZnCh (1.36–1.45 eV).[35] The number of reduced double bonds in the pyrrole rings is zero in the case of porphyrins, one in the case of chlorins and two diagonal to each other in the case of bacteriochlorins. The ionization potentials of the tetrapyrroles decrease with increasing peripheral saturation,[39] consistent with the electrochemical data. This may be the reason why natural photosynthesis utilizes chlorophylls rather than porphyrins as antenna molecules. In any case, the energy level of the radical ion pair in reference to the triplet energy of a component is an important factor in determining the lifetime of the radical ion pair.

The fate of the charge-separated state of porphyrin linked C_{60} can also be altered by modifying substituents on the porphyrin ring. When ZnP (P^{2-} = 5,10,15,20-tetrakis(3,5-di-*tert*-butylphenyl)porphyrin dianion) is employed to link with C_{60}, the radical ion pair state ($ZnP^{\bullet+}$–$C_{60}^{\bullet-}$) is lower in energy (1.38 eV) than both the triplet excited state of C_{60} and ZnP to afford a sufficiently long lifetime (0.77 μs) for a subsequent charge-separation step.[37] A series of porphyrin–fullerene linked molecules with the same spacer as employed for ZnP–C_{60} (R_{ee} = 11.9 Å) has been synthesized; Fc–ZnP–C_{60} (R_{ee} = 30.3 Å), ZnP–H_2P–C_{60} (R_{ee} = 30.3 Å), and Fc–ZnP–H_2P–C_{60} (R_{ee} = 48.9 Å) as shown in Fig. 4.[37,38] The driving force dependence of the electron transfer rate constants (k_{ET}) of these dyad, triads and tetrad molecules is shown in Fig. 5, where log k_{ET} is plotted against the driving force ($-\Delta G^0_{ET}$).[38] The lines in Fig. 5 represent the best fit to eqn. (6) (ZnP–C_{60}: λ = 0.66 eV, V = 3.9 cm^{-1}; Fc–ZnP–C_{60}, Fc–H_2P–C_{60}, and ZnP–H_2P–C_{60}: λ = 1.09 eV, V = 0.019 cm^{-1}; Fc–ZnP–H_2P–C_{60}: λ = 1.32 eV, V = 0.00017 cm^{-1}).[37,38] The λ value increases whereas the V value decreases with increasing edge-to-edge distance in the order of the dyad (R_{ee} = 11.9 Å), the triads (R_{ee} = 30.3 Å) and tetrad (R_{ee} = 48.9 Å). In the case of the dyad, the CR rate in $ZnP^{\bullet+}$–$C_{60}^{\bullet-}$ is much slower than the CS rate constants from both the singlet and triplet excited states (Fig. 5). This enables a subsequent electron transfer from Fc to $ZnP^{\bullet+}$ in the triad (Fc–$ZnP^{\bullet+}$–$C_{60}^{\bullet-}$) and from ZnP to $H_2P^{\bullet+}$ in ZnP–$H_2P^{\bullet+}$–$C_{60}^{\bullet-}$ to produce the charge separated state, Fc^+–ZnP–$C_{60}^{\bullet-}$ and $ZnP^{\bullet+}$–H_2P–$C_{60}^{\bullet-}$, in competition with the back electron transfer in the initial CS states. In the case of the tetrad (Fc–ZnP–H_2P–C_{60}), the multi-step electron transfer processes (Scheme 2) afford the final CS state, Fc^+–ZnP–H_2P–$C_{60}^{\bullet-}$, in which charges are separated at a long distance (R_{ee} = 48.9 Å).[38] The lifetime of the resulting charge-separated state at a long distance in a frozen PhCN has been determined to be as long as 0.38 s and is comparable to that observed for the bacterial photosynthetic reaction center.[38] Such an extremely long lifetime of a CS state could only be determined in frozen media, since in condensed media bimolecular back electron transfer between two Fc^+–ZnP–H_2P–$C_{60}^{\bullet-}$ is much faster than the unimolecular CR process.[38] The maximum k_{ET} value ($k_{ET,max}$) of each Marcus plot in Fig. 5 is correlated with the edge-to-edge distance (R_{ee}), separating the radical ions, according to eqn. (7):[38]

$$\ln k_{ET,max} = \ln\left(\frac{2\pi^{3/2} V_0^2}{h\,(\lambda k_B)^{1/2}}\right) - \beta R_{ee} \qquad (7)$$

Hereby, V_0 refers to the maximal electronic coupling element, while β is the decay coefficient factor (damping factor), which depends primarily on the nature of the bridging molecule. From the linear plot of ln $k_{ET,max}$ *vs.* R_{ee} the β value is obtained as 0.60 $Å^{-1}$.[38] This β value is located within the boundaries of nonadiabatic electron transfer reactions for saturated

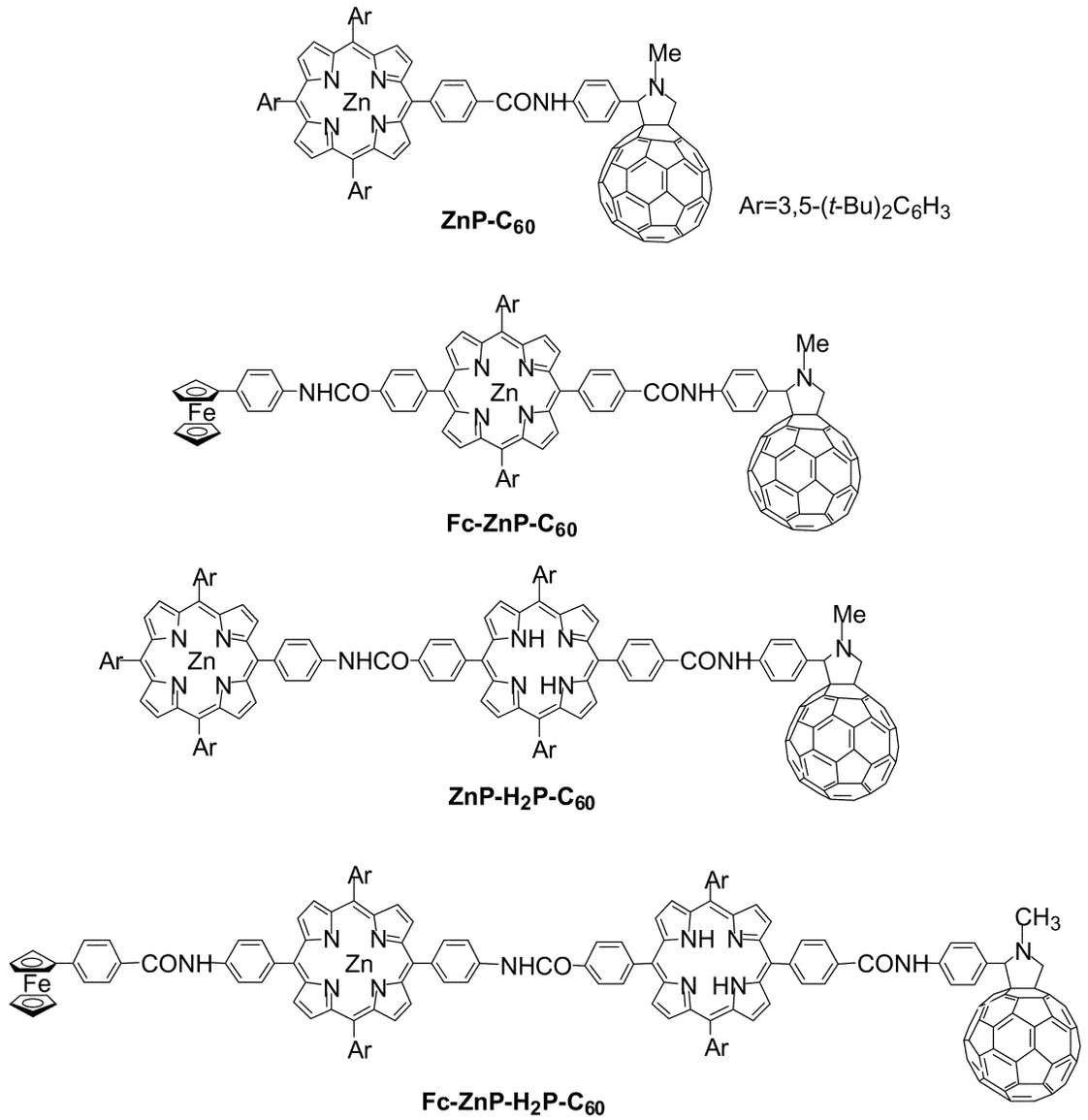

Fig. 4 Structures of a series of porphyrin–fullerene linked molecules.[34]

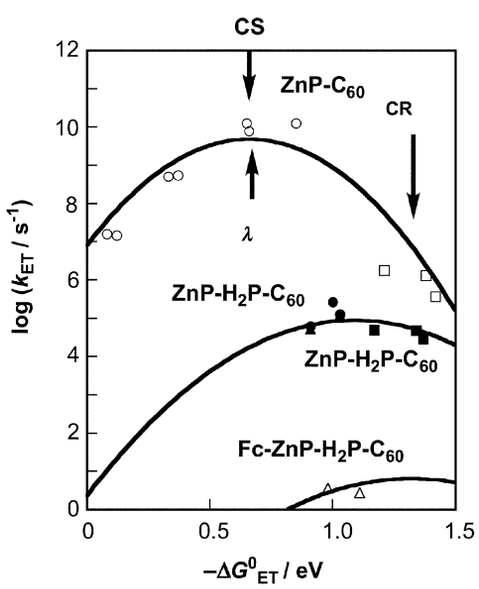

Fig. 5 Driving force ($-\Delta G^0_{ET}$) dependence of intramolecular ET rate constants in ZnP–C_{60} (CS: open circles; CR: open squares), Fc–ZnP–C_{60} (solid circles), Fc–H_2P–C_{60} (solid triangles), ZnP–H_2P–C_{60} (solid squares), and Fc–ZnP–H_2P–C_{60} (open triangles).[38]

hydrocarbon bridges (0.8–1.0 $Å^{-1}$) and unsaturated phenylene bridges (0.4 $Å^{-1}$).[40]

According to eqn. (7), the electron transfer rate constant falls off exponentially with increasing distance between the donor and acceptor molecules provided that the other parameters such as the driving force and reorganization energy of electron transfer remain the same. Thus, the time scale of electron transfer is expected to increase from femtoseconds to hours and even to days by simply increasing the distance. However, such an extremely slow electron transfer at a long distance is difficult to observe because the electron transfer reactions at fixed distances mentioned above involve the excited state and the inherent short lifetime has precluded the study on an extremely slow electron transfer processes.

A slow thermal electron transfer would only be achieved if an electron donor or acceptor molecule is encapsulated in a large inert environment which prohibits the close access of the other molecule. Such encapsulation of chromophore ions in the supercage of zeolites has been utilized to retard the back electron transfer across the zeolite–solution interface in photoinduced charge separation systems.[41] On the other hand, addition of an electron donor which cannot penetrate into the zeolite supercage to the acceptor-encapsulated zeolite can start the thermal electron transfer at long distances through the zeolite–solution interface. An extremely slow electron transfer

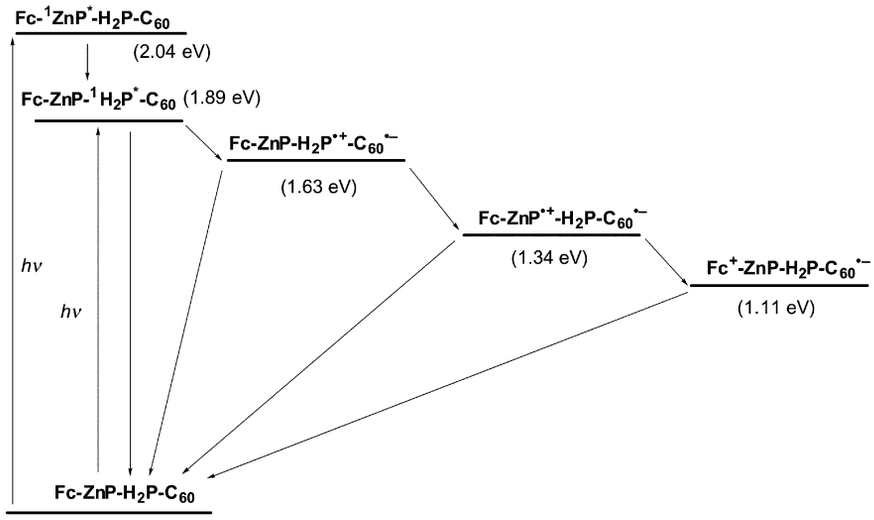

Scheme 2 Reaction scheme and energy diagram for Fc–ZnP–H_2P–C_{60} in PhCN.[38]

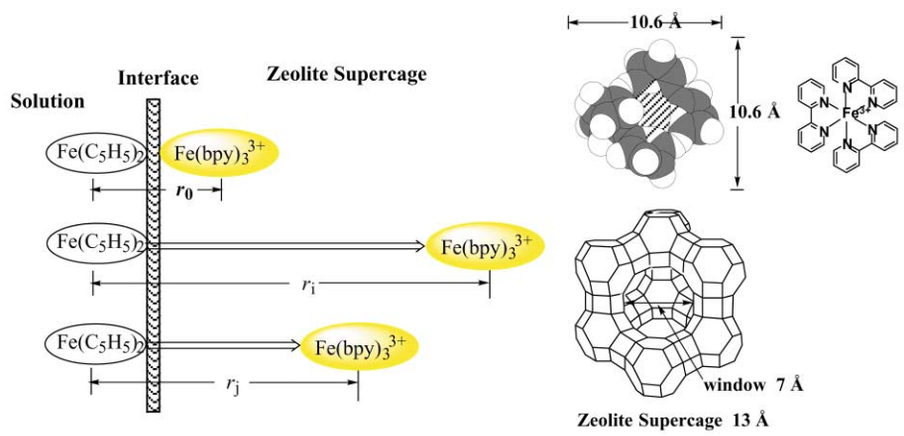

Scheme 3 Schematic diagram for electron transfer from an electron donor (ferrocene) to $Fe(bpy)_3^{3+}$ incorporated inside the Y type zeolite through the zeolite–solution interface.[42]

from an electron donor to $Fe(bpy)_3^{3+}$ incorporated inside the Y type zeolite is reported to occur through the zeolite–solution interface such that the completion of electron transfer takes days in sharp contrast to the corresponding electron transfer reaction in solution, which is too fast to be followed even by using a stopped-flow technique.[42] Such an extremely slow electron transfer is ascribed to a very long-range electron transfer from adsorbed ferrocene molecules across the zeolite–solution interface to $Fe(bpy)_3^{3+}$ inside the zeolite supercage at various distances (Scheme 3). The electron transfer rate constants of various electron donors at an averaged distance (k_{ETav}) have been determined by analyzing a dispersion of r according to a normal Gaussian distribution.[42] Electron donors are chosen such that the reorganization energies of electron transfer are similar to the value of $Fe(C_5H_5)_2^+/Fe(C_5H_5)_2$ (1.01 eV). A plot of log k_{ETav} *vs.* $-\Delta G^0_{ET}$ in Fig. 6 exhibits a Marcus parabolic dependence of log k_{ETav} on $-\Delta G^0_{ET}$ as expected from eqn. (6). Using a typical β value for through space electron transfer in solution (1.2 Å^{-1}), the average distance ($r - r_0$) for electron transfer from $Fe(C_5H_5)_2$ to $Fe(bpy)_3^{3+}$–zeolite Y is roughly evaluated as 41 Å which corresponds to the distance across three supercages.[42]

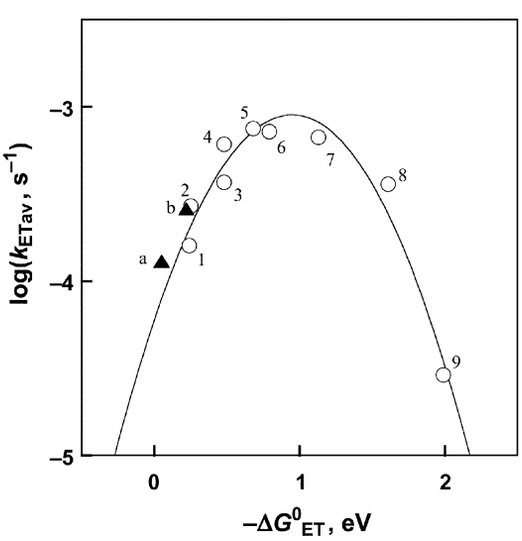

Fig. 6 Dependence of averaged electron transfer rate constants (k_{ETav}) on driving force ($-\Delta G^0_{ET}$) of electron transfer in deaerated MeCN at 298 K.[42] Open circles: Electron transfer from donor to $Fe(bpy)_3^{3+}$–Y (1: $Fe(C_5H_4COCH_3)_2$, 2: $AcrH_2$, 3: $Fe(C_5H_5)(C_5H_4COCH_3)$, 4: BNAH, 5: $Fe(C_5H_5)_2$, 6: $Fe(C_5H_4Me)_2$, 7: $Fe(C_5Me_5)_2$, 8: $Mn(C_5Me_5)_2$, 9: $Co(C_5H_5)_2$). Solid triangles: Electron transfer from $Fe(bpy)_3^{2+}$–Y to acceptor (a: $Ru(Me_2bpy)_3^{3+}$, b: $Ru(bpy)_3^{3+}$).

4 Lewis acid promoters for electron transfer reduction of oxygen

As described above, the rates of electron transfer can be finely controlled by the fundamental electron transfer properties of electron donors and acceptors (the redox potentials and the reorganization energies) and also by the electron donor–acceptor distance and the environment surrounding them. In other words, the electron transfer reactivity is fixed once an

electron donor–acceptor pair is chosen in a certain environment. However, the electron transfer reactivity can be altered by addition of a third component which can change the fundamental electron transfer properties of electron donors or acceptors. The most important substrate in such a case is oxygen, which is reduced by the function of metalloenzymes in respiration. Since the ground state oxygen is triplet, the direct reaction of oxygen with singlet molecules to produce singlet oxygenated product is spin-forbidden, whereas an electron transfer from a singlet electron donor to oxygen is a spin-allowed process. Thus, the activation of oxygen should involve the electron transfer reduction. However, O_2 is rather difficult to reduce by electron transfer because of the largely negative one-electron reduction potential.[43] When the one-electron oxidation potential of an electron donor (D) is more positive than the one-electron reduction potential of O_2, the electron transfer is endergonic and thereby no net electron transfer takes place.

In the presence of metal ions which are Lewis acids and can bind with $O_2^{\bullet-}$, however, the free energy change of electron transfer would be negative provided that the binding energy between $O_2^{\bullet-}$ and the metal ions is large enough. In fact, a variety of metal ions (M^{n+}) are known to bind with $O_2^{\bullet-}$.[44] The g_{zz}-value of the EPR spectrum of the $O_2^{\bullet-}$–M^{n+} complex varies depending on the type of metal ion.[45] The deviation of the g_{zz}-value from the free spin value ($g_e = 2.0023$) is caused by the spin–orbit interaction as given by eqn. (8) under the conditions that $\Delta E \gg \lambda$, where λ is the spin–orbit coupling constant (0.014 eV) and ΔE is the energy splitting of π_g levels due to the complex formation between $O_2^{\bullet-}$ and M^{n+}.[45] The ΔE value is readily determined from the g_{zz}-value using eqn. (8).

$$g_{zz} = g_e + 2\lambda/\Delta E \qquad (8)$$

The ΔE value can be used to predict the promoting effect of M^{n+} on electron transfer from CoTPP (TPP^{2-} = tetraphenylporphyrin dianion) to O_2 in MeCN at 298 K (Scheme 4).[45] Electron transfer from CoTPP to O_2 occurs efficiently in the presence of metal ion salts which can bind with $O_2^{\bullet-}$, whereas no electron transfer from CoTPP to O_2 occurs in the absence of metal ion. This is because the electron transfer is highly endergonic judging from the one-electron oxidation potential of CoTPP ($E^0_{ox} = 0.35$ V *vs.* SCE in MeCN) and the one-electron reduction potential of O_2 ($E^0_{red} = -0.87$ V *vs.* SCE).[45] In the presence of metal ions, the E^0_{red} value of O_2 is shifted to a positive direction due to the binding of $O_2^{\bullet-}$ with metal ions, when electron transfer from CoTPP to O_2 becomes exergonic. The observed second-order rate constant of electron transfer ($dm^3\ mol^{-1}\ s^{-1}$) increases linearly with increasing metal ion concentration. From the slope of the linear correlation is obtained the metal ion-promoted electron transfer rate constant ($k_{et}/dm^6\ mol^{-2}\ s^{-1}$). There is a striking single linear correlation between log k_{et} and ΔE of the $O_2^{\bullet-}$ complexes with not only metal ions (triflate or perchlorate salts) but also organotins which are often used as Lewis acids to promote C–C bond formation in organic synthesis, as shown in Fig. 7.[45,46] The remarkable correlation spans a range of almost 10^7 in the rate constant. The slope of the linear correlation between log k_{et} and ΔE is obtained as 14.0 which is close to the value of $1/2.3k_BT$ (= 16.9 at 298 K). This means that the variation of ΔE is well reflected in the difference in the activation free energy for the Lewis acid-promoted electron transfer from CoTPP to O_2. The

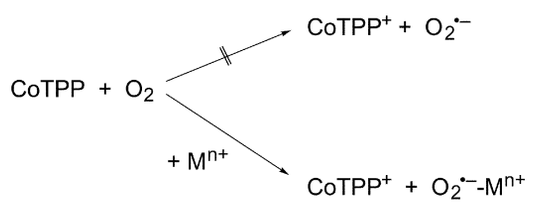

Scheme 4 Metal ion-promoted electron transfer from CoTPP to O_2.

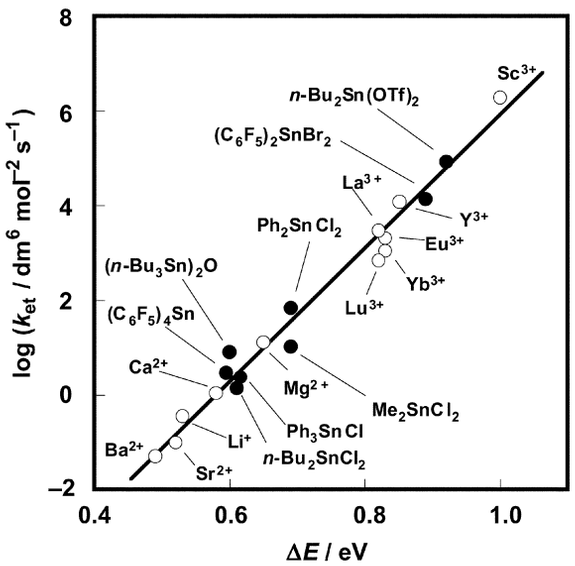

Fig. 7 Plots of log k_{et} *vs.* ΔE in electron transfer from (TPP)Co to O_2, promoted by metal ions (triflate or perchlorate salts) (○) and organotin compounds (●) in MeCN at 298 K.[46]

stronger the binding of the Lewis acid with $O_2^{\bullet-}$, the larger will be the promoting effect of metal ions and organotins. Scandium triflate [$Sc(OTf)_3$] is the strongest Lewis acid examined, exhibiting the largest promoting effect on the electron transfer reduction of O_2 (Fig. 7). Thus, ΔE can be regarded as a good measure of the binding energies in $O_2^{\bullet-}$ complexes with metal ions and organotins. However, this method can only be applied to diamagnetic metal ions, since the paramagnetic metal ion-$O_2^{\bullet-}$ complexes give no EPR signal. Redox active metal ions which undergo electron transfer reactions with $O_2^{\bullet-}$ cannot be employed, either.

A more convenient method to provide a quantitative measure of the Lewis acidity of metal ion salts has been reported using the fluorescence maxima of 10-methylacridone (AcrCO)–metal ion salt complexes [eqn. (9)].[47,48] The florescence energy (hv_f) decreases with increasing Lewis acidity of the metal ion salts. There is a striking linear correlation between the hv_f values of ^{1}AcrCO*–Lewis acid complexes and the ΔE values of the $O_2^{\bullet-}$–Lewis acid complexes derived from the g_{zz}-values as shown in Fig. 8, where the two parallel correlations correspond to the energy splitting due to the coupling of CO stretching in the ^{1}AcrCO*–M^{n+} complex.[48] The stronger the acidity of the Lewis acid, the larger is the ΔE value, the more red-shifted is the λ_{max}

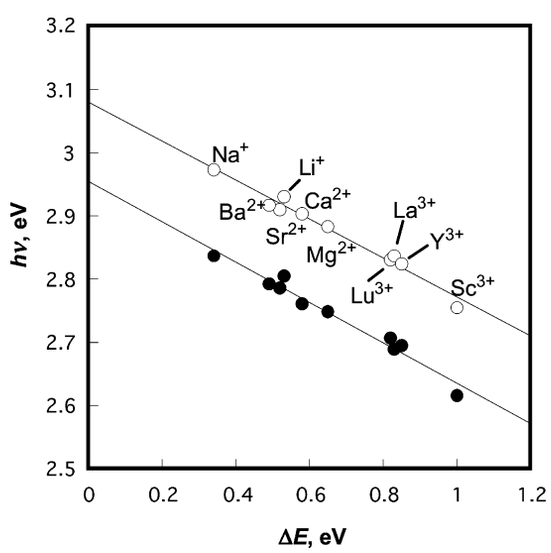

Fig. 8 Plots of hv_f of the ^{1}AcrCO*–M^{n+} complexes *vs.* ΔE of the $O_2^{\bullet-}$–M^{n+} complexes in MeCN 298 K.[48]

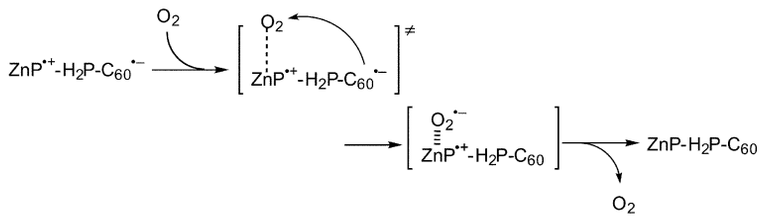

Scheme 5 Catalysis of O_2 in back electron transfer in ZnP-linked C_{60}.[49]

value, and the smaller is the $h\nu_f$ value. The good linear correlation between ΔE and $h\nu_f$ (Fig. 8) demonstrates that the $h\nu_f$ values provide a convenient quantitative measure of Lewis acidity of all kinds of metal ion salts including paramagnetic and redox active Lewis acids. Using the quantitative measure of the Lewis acidity of metal ion salts, the promoting effects of variety of Lewis acids on the electron transfer reduction of O_2 can be well predicted (Fig. 7).

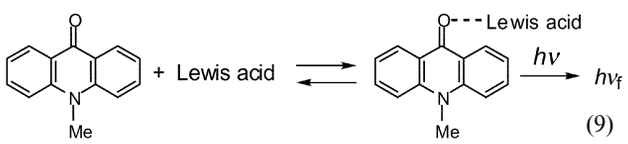

(9)

The promoting effect of metal ions on the electron transfer reduction of O_2 has been reported to result in a novel catalytic effect of O_2 on the back electron transfer process in the CS state of ZnP–C_{60}.[49] In the presence of oxygen, the lifetimes of both radical ion pairs (*i.e.*, $ZnP^{\bullet+}$–$C_{60}^{\bullet-}$ and $ZnP^{\bullet+}$–H_2P–$C_{60}^{\bullet-}$) are decreased significantly due to an oxygen-catalyzed back electron transfer between $C_{60}^{\bullet-}$ and $ZnP^{\bullet+}$.[49] The catalytic participation of O_2 in an intramolecular back electron transfer between $C_{60}^{\bullet-}$ and $ZnP^{\bullet+}$ in ZnP-linked C_{60} is depicted in Scheme 5.[49] The intermolecular electron transfer from $C_{60}^{\bullet-}$ to O_2 is facilitated by the binding of $O_2^{\bullet-}$ with the Zn(II) ion of $ZnP^{\bullet+}$, which is followed by a rapid intramolecular electron transfer from $O_2^{\bullet-}$ to $ZnP^{\bullet+}$ in the $O_2^{\bullet-}$–$ZnP^{\bullet+}$ complex to regenerate O_2.[49]

The binding of $O_2^{\bullet-}$ with Zn(II) ions also plays an important role not only in the electron transfer reduction of $O_2^{\bullet-}$ but also in the further reduction of $O_2^{\bullet-}$. The superoxide ion ($O_2^{\bullet-}$) produced by the electron transfer reduction of O_2 is toxic, causing oxidative damage to cells and therefore is removed by copper–zinc superoxide dismutase (Cu,Zn–SOD) which catalyzes the disproportionation (dismutation) of $O_2^{\bullet-}$ to O_2 and H_2O_2.[50] The important role of Zn(II) in the bimetallic system to activate both the oxidation and reduction of $O_2^{\bullet-}$ has been revealed by a well-characterized SOD model, that is an imidazolate-bridged Cu(II)–Zn(II) heterodinuclear complex containing a dinucleating ligand, Hbdpi (Hbdpi = 4,5-bis(bis(2-pyridylmethyl)aminomethyl)imidazole).[51–53] The crystal structure is shown in Fig. 9, where the Cu(II)–Zn(II) distance of 6.197(2) Å in the Cu(II)–Zn(II) heterodinuclear complex agrees well with that of native Cu,Zn–SOD (6.2 Å), and each metal has the pentacoordinate geometry with the imidazolate nitrogen, two pyridine nitrogens, the tertiary amine nitrogen, and a solvent (MeCN or H_2O). The

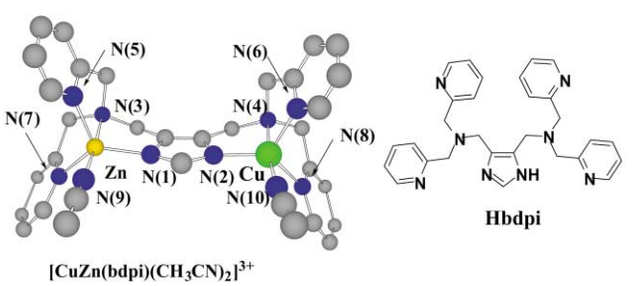

Fig. 9 Crystal structure of a SOD model complex, $[CuZn(bdpi)(CH_3CN)_2]^{3+}$.[51]

Cu(II)–Zn(II) SOD model complex has a coordination site available for the binding of $O_2^{\bullet-}$ (Fig. 9). The Cu(I)–Zn(II) heterodinuclear complex exhibits the highest catalytic activity toward the dismutation of $O_2^{\bullet-}$.[51] A large positive shift (about 0.2 V) in the $E_{1/2}$ value of the Cu(II)–Zn(II) complex is observed due to the electron withdrawing effects of the Zn(II) ion as compared to the corresponding Cu(II) mononuclear complexes.[51] This indicates that an important role of the Zn(II) ion in the imidazolate-bridged Cu(II)–Zn(II) complex is to accelerate an outer-sphere electron transfer from $O_2^{\bullet-}$ to produce the Cu(I)–Zn(II) complex, when the free energy change of electron transfer to Cu(II) becomes thermodynamically more favorable as compared to that without the Zn(II) ion. The presence of Zn(II), which can act as a Lewis acid, is also able to accelerate an electron transfer from the Cu(I)–Zn(II) complex to $O_2^{\bullet-}$, since $O_2^{\bullet-}$ can bind with a Zn(II) ion acting as a Lewis acid to accelerate the electron transfer reduction of $O_2^{\bullet-}$ (*vide supra*). Thus, the essential role of Zn(II) ions in SODs may be to accelerate both the oxidation and reduction of $O_2^{\bullet-}$ by controlling the redox potentials of Cu(II) ions and $O_2^{\bullet-}$ in the catalytic cycle of SOD as shown in Scheme 6.[51–53]

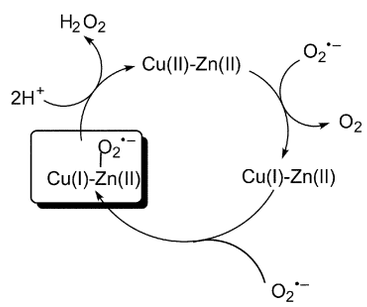

Scheme 6 Catalytic mechanism of SOD.[51–53]

5 Promoting effects of metal ions and hydrogen bonding on thermal intramolecular electron transfer

An intramolecular electron transfer reaction of a donor–acceptor linked system can also be promoted by addition of a metal ion.[54] Addition of scandium triflate [$Sc(OTf)_3$] to an MeCN solution of ferrocene–naphthoquinone dyad (Fc–NQ) results in intramolecular electron transfer from Fc to NQ to form the Fc^+–$NQ^{\bullet-}$/Sc^{3+} complex as indicated by the appearance of the absorption band due to the Fc^+ moiety at 860 nm together with the absorption band at λ_{max} = 420 nm due to the $NQ^{\bullet-}$/Sc^{3+} moiety (Scheme 7).[54] The electron transfer from Fc to NQ is made possible by the binding of Sc^{3+} with $NQ^{\bullet-}$ together with the hydrogen bonding between the amide proton and the carbonyl oxygen of $NQ^{\bullet-}$.[54]

The effect of hydrogen bonding on metal ion-promoted electron transfer has been quantitatively evaluated using a ferrocene–*p*-benzoquinone dyad (Fc–Q) in comparison with the Fc–(Me)Q dyad, in which the N–H group acting as a hydrogen-bond acceptor, is replaced by N–Me (Scheme 8).[55] The promoting effects of metal ions vary significantly depending on the Lewis acidity of metal ions (M^{n+}). The k_{ET} values of M^{n+}-promoted electron transfer in Fc–Q are linearly correlated with the ΔE values of the $O_2^{\bullet-}$-Lewis acid complexes (*vide supra*) and

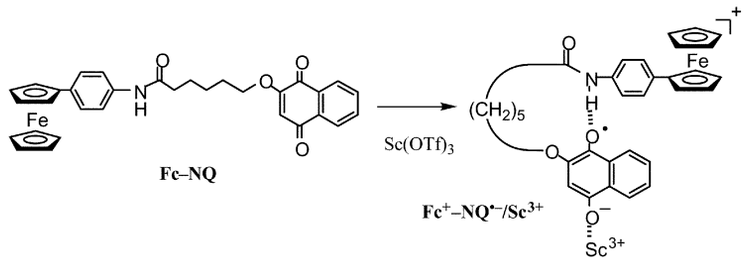

Scheme 7 Sc^{3+}-promoted intramolecular electron transfer from Fc to NQ in the Fc–NQ dyad.[54]

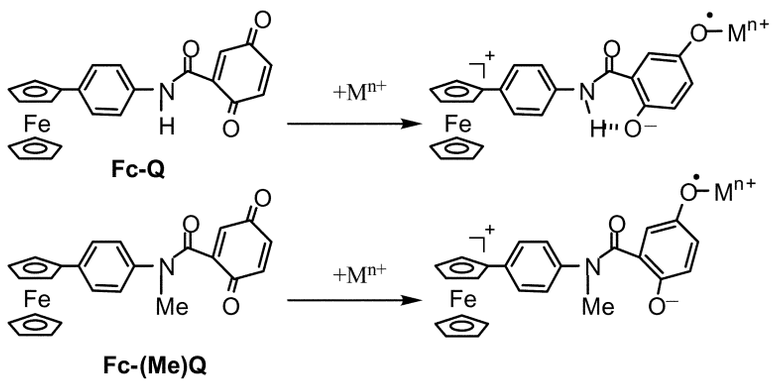

Scheme 8 M^{n+}-promoted electron transfer in the Fc–Q and Fc–(Me)Q dyads.

each value is *ca.* 10^4 times larger than the k_{ET} values of Fc–(Me)Q as shown in Fig. 10.[55] The 10^4 times difference in the k_{ET} values corresponds to the difference in the one-electron reduction potential between Fc–Q (E^0_{red} *vs.* SCE = −0.16 V) and Fc–(Me)Q (E^0_{red} *vs.* SCE = −0.40 V). The stabilization of the $Q^{\bullet-}$ moiety by hydrogen bonding with the amide proton in Fc–$Q^{\bullet-}$ results in the positive shift in E^0_{red} of Fc–Q as compared to Fc–(Me)Q in which the amide proton is replaced by the methyl group. Thus, the remarkable difference in the k_{ET} values between Fc–Q and Fc–(Me)Q is ascribed to the effect of the hydrogen bond formed between the $Q^{\bullet-}$ moiety and the amide proton in Fc^+–$Q^{\bullet-}$.

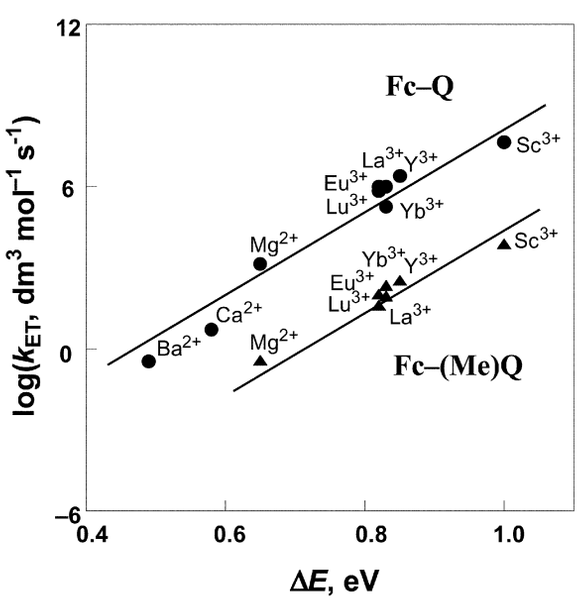

Fig. 10 Plots of log k_{ET} *vs.* ΔE in M^{n+}-promoted electron transfer in Fc–Q and Fc–(Me)Q in MeCN 298 K.[55]

In the case of the photoinduced electron in the Fc–Q dyad, however, electron transfer from Fc to the singlet excited state of Q occurs rapidly to produce Fc–$Q^{\bullet-}$ without changing the conformation (< 1 ps) and then $Q^{\bullet-}$ forms the hydrogen bond with the amide proton of the spacer (τ = ~5 ps) as shown in Scheme 9.[56] When photoinduced electron transfer is thermodynamically feasible without the help of hydrogen bonding, electron transfer precedes the hydrogen bond formation (Scheme 9) in contrast with the case of metal ion-promoted electron transfer in which the hydrogen bond formation is coupled with the electron transfer (Scheme 8).

6 C–C bond formation *via* metal ion-promoted electron transfer

The promoting effects of metal ions on electron transfer have been utilized for their catalytic effects on overall chemical transformation in which the metal ion-promoted electron transfer is the rate-determining step. The Mg^{2+}-catalyzed hydride transfer from an NADH (dihydronicotinamide adenine dinucleotide) model compound, 1-benzyl-1,4-dihydronicotinamide (BNAH), to Q is known to proceed *via* a Mg^{2+}-promoted electron transfer from BNAH to Q, followed by a proton transfer from the resulting $BNAH^{\bullet+}$ to the $Q^{\bullet-}$–Mg^{2+} complex and the subsequent fast electron transfer from $BNA^{\bullet}$ to QH^-–Mg^{2+}.[57] When BNAH is replaced by 1-benzyl-4-*t*-butyl-1,4-dihydronicotinamide (*t*-BuBNAH), no reaction occurs between *t*-BuBNAH and Q in a deaerated MeCN. In the presence of $Sc(OTf)_3$, the Lewis acidity of which is much stronger than Mg^{2+}, however, cycloaddition reaction of *t*-BuBNAH with Q rather than hydride transfer occurs efficiently at 298 K [eqn. (10)].[58]

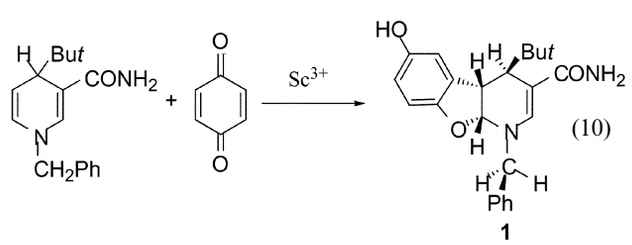

(10)

The Sc^{3+}-catalyzed cycloaddition of Q also occurs with BNAH.[58] Kinetic comparison between the Sc^{3+}-catalyzed cycloaddition and the Sc^{3+}-promoted electron transfer reduction of Q together with the absence of the deuterium kinetic

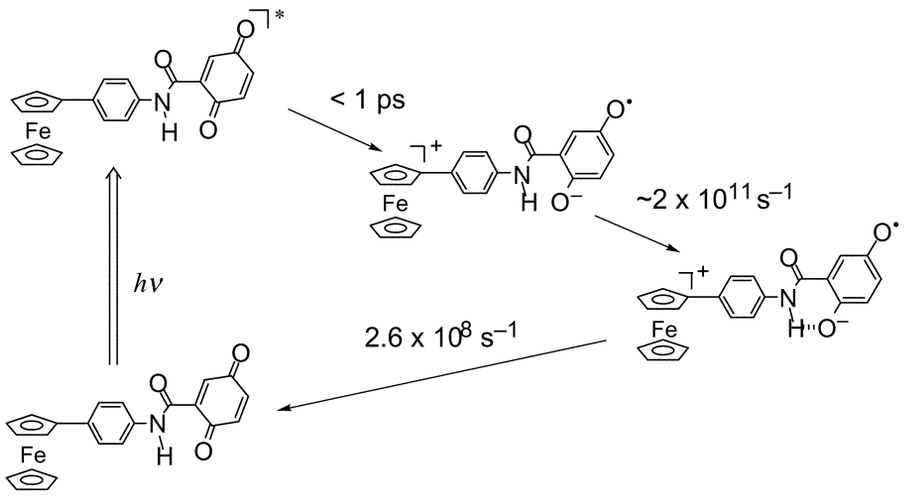

Scheme 9 Photoinduced electron transfer of Fc–Q and subsequent hydrogen bond formation.[55,56]

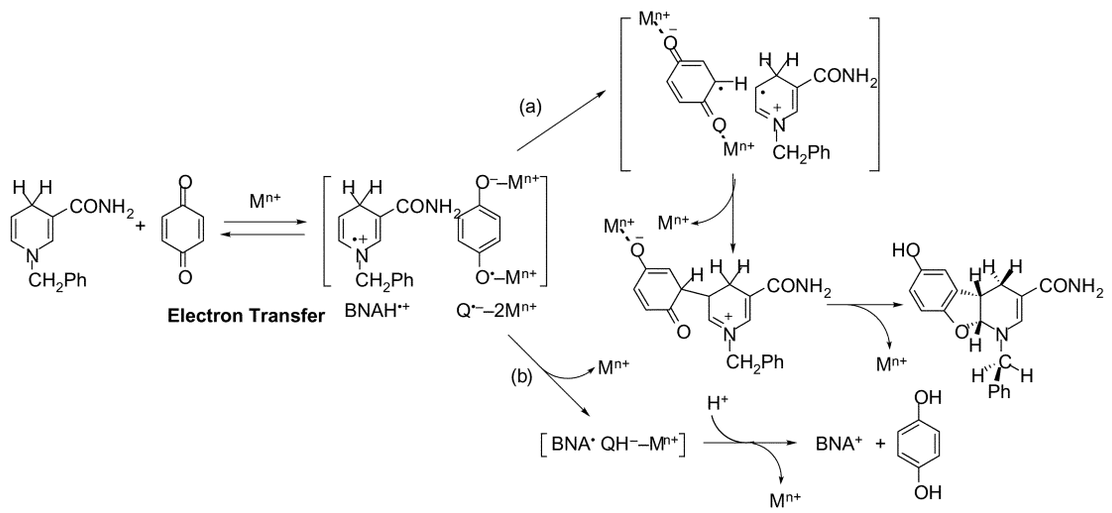

Scheme 10 Mechanism of M^{n+}-catalyzed reaction of BNAH with Q.[58]

isotope effect indicates that the C–C bond formation proceeds *via* the Sc^{3+}-promoted electron transfer from *t*-BuBNAH and BNAH to Q.[58] The change in the type of reaction depending on the Lewis acidity of the metal ion is well explained by the electron transfer mechanism in Scheme 10.[58] The initial rate-determining electron transfer from BNAH to Q results in the formation of a radical ion pair ($BNAH^{\bullet+}$ and $Q^{\bullet-}$) where $Q^{\bullet-}$ forms 1:1 and 1:2 complexes with Sc^{3+}. The formation of such a 1:2 complexes between $Q^{\bullet-}$ and Sc^{3+} has been confirmed by the EPR spectrum which exhibits superhyperfine structure due to the interaction of an unpaired electron with two equivalent Sc^{3+} nuclei.[58,59] The proton transfer from $BNAH^{\bullet+}$ to the $Q^{\bullet-}$–$2Sc^{3+}$ complex may be retarded because of the strong Lewis acidity of Sc^{3+}. In such a case the initial electron transfer is followed by the radical coupling (C–C bond formation) between $Q^{\bullet-}$ and $BNAH^{\bullet+}$ to give the zwitterionic intermediate which is eventually converted to the cycloadduct (Scheme 10a). The proton transfer from $BNAH^{\bullet+}$ to the $Q^{\bullet-}$–$2M^{n+}$ complex accelerates with decreasing Lewis acidity of the metal ion (M^{n+}) due to the stronger basicity of the $Q^{\bullet-}$–$2M^{n+}$ complex (Scheme 10b).

This is the reason why the hydride transfer pathway from BNAH to Q becomes dominant in the presence of a much weaker Lewis acid (*e.g.*, Mg^{2+}) as compared with the selective cycloaddition reaction in the presence of Sc^{3+}. Thus, the Lewis acidity of the metal ion can control the transfer step and also the subsequent chemical step.

The radical cation of an NADH model compound ($BNAH^{\bullet+}$), a reactive radical intermediate in Scheme 10, has recently been detected by EPR which confirms that the keto form in Scheme 10 is thermodynamically more stable than the enol isomeric form.[60]

Rates of Diels–Alder cycloaddition of anthracenes with *p*-benzoquinone and its derivatives as well as rates of hydride transfer reactions from 10-methyl-9,10-dihydroacridine ($AcrH_2$) to the same series of *p*-benzoquinones are also accelerated significantly in the presence of metal ions in MeCN.[61,62] Extensive comparison of the catalytic effects of metal ions in electron transfer from one-electron reductants (cobalt tetraphenylporphyrin and decamethylferrocene) to *p*-benzoquinones with those in the Diels–Alder reactions of the quinones as well as the hydride transfer reactions has revealed that the catalysis of metal ions in each case is ascribed to the 1:1 and 1:2 complexes formed between the corresponding semiquinone radical anions and metal ions as in the case of the metal ion-catalyzed hydride transfer and cycloaddition reactions of BNAH with Q.[62] The catalytic reactivities of a variety of metal ions in each reaction are well correlated with the ΔE values in Fig. 7.[62] Hydride transfer from $AcrH_2$ to 3,6-diphenyl-1,2,4,5-tetrazine (Ph_2Tz) which contains N=N double bond also occurs efficiently in the presence of $Sc(OTf)_3$ *via* Sc^{3+}-promoted electron transfer from $AcrH_2$ to Ph_2Tz in MeCN at 298 K, whereas no reaction occurs in the absence of Sc^{3+}.[63]

7 Conclusion and perspectives

Efficient multi-step electron transfer systems have been designed using suitable components based on the Marcus theory of electron transfer to mimic the function of a

photosynthetic reaction center. The concept of catalytic control of electron transfer reactions provides a new perspective of electron transfer chemistry, expanding the scope of electron transfer systems which would otherwise be impossible to study. It has been demonstrated that binding of a metal ion with the substrate radical anion plays an important role in the catalytic control of electron transfer reactions. The promoting effects of metal ions on the electron transfer reactions are related to the Lewis acidity of metal ions which can be evaluated quantitatively based on the g_{zz}-values of the EPR spectra of metal ion-$O_2^{\bullet -}$ complexes as well as the fluorescence maxima of 10-methylacridone (AcrCO)–metal ion salt complexes. The Lewis acidity of metal ions has been shown to control not only the electron transfer step but also the subsequent chemical step in the overall chemical reactions. However, there still remains a wealth of important fundamental questions with regard to catalytic control of electron transfer reactions, which have been only partially explored so far. Catalysis in chemical transformation involving the rate-determining electron transfer certainly deserves much more detailed attention in future.

Acknowledgements

The author gratefully acknowledges the contributions of many collaborators and coworkers mentioned in the references, in particular Prof. H. Imahori (Kyoto University), Prof. O. Ito (Tohoku University), Dr D. M. Guldi (University of Notre Dame), Dr T. Suenobu, Dr K. Ohkubo and Mr K. Okamoto (Osaka University). The authors acknowledge continuous support of their study by a Grant-in-Aid from the Ministry of Education, Science, Culture and Sports, Japan.

References

1 (*a*) R. A. Marcus, *Annu. Rev. Phys. Chem.*, 1964, **15**, 155; (*b*) R. A. Marcus and N. Sutin, *Biochim. Biophys. Acta*, 1985, **811**, 265; (*c*) R. A. Marcus, *Angew. Chem. Int. Ed. Engl.*, 1993, **32**, 1111.
2 *Electron Transfer in Chemistry*, ed. V. Balzani, Wiley-VCH, Weinheim, 2001, vol. 4, pp. 3–67.
3 (*a*) A. Weller and K. Zacharaasse, *Chem. Phys. Lett.*, 1971, **10**, 590; (*b*) P. Suppan, *Top. Curr. Chem.*, 1992, **163**, 95; (*c*) B. S. Brunschwig, S. Ehrenson and N. Sutin, *J. Am. Chem. Soc.*, 1984, **106**, 6858; (*d*) A. V. Barzykin, P. A. Frantsuzov, K. Seki and A. Tachiya, *Adv. Chem. Phys.*, 2002, **123**, 511.
4 (*a*) C. Turró, J. M. Zaleski, Y. M. Karabatsos and D. G. Nocera, *J. Am. Chem. Soc.*, 1996, **118**, 6060; (*b*) K. Ishiguro, T. Nakano, H. Shibata and Y. Sawaki, *J. Am. Chem. Soc.*, 1996, **118**, 7255; (*c*) P. Thanasekaran, T. Rajendran, S. Rajagopal, C. Srinivasan, R. Ramaraj, P. Ramamurthy and B. Venkatachlapathy, *J. Phys. Chem. A*, 1997, **101**, 8195.
5 (*a*) C. Li and M. Z. Hoffman, *J. Phys. Chem. A*, 1998, **102**, 6052; (*b*) H. Yokoi, S. Moriizumi, K. Ishiguro and Y. Sawaki, *J. Photochem. Photobiol. A*, 1999, **125**, 39.
6 M. A. Smitha, E. Prasad and K. R. Gopidas, *J. Am. Chem. Soc.*, 2001, **123**, 1159.
7 (*a*) A. Rehm and A. Weller, *Ber. Bunsenges Phys. Chem.*, 1969, **73**, 834; (*b*) A. Rehm and A. Weller, *Isr. J. Chem.*, 1970, **8**, 259.
8 (*a*) C. R. Bock, T. J. Meyer and D. G. Whitten, *J. Am. Chem. Soc.*, 1975, **97**, 2909; (*b*) R. Ballardini, G. Varani, M. T. Indelli, F. Scandola and V. Balzani, *J. Am. Chem. Soc.*, 1978, **100**, 7219; (*c*) S. Fukuzumi, S. Kuroda and T. Tanaka, *J. Am. Chem. Soc.*, 1985, **107**, 3020; (*d*) S. Fukuzumi, S. Koumitsu, K. Hironaka and T. Tanaka, *J. Am. Chem. Soc.*, 1987, **109**, 305; (*e*) S. S. Jayanthi and P. Ramamurthy, *J. Phys. Chem. A*, 1997, **101**, 2016.
9 S. Fukuzumi, K. Ohkubo, T. Suenobu, K. Kato, M. Fujitsuka and O. Ito, *J. Am. Chem. Soc.*, 2001, **123**, 8459.
10 (*a*) G. L. Closs and J. R. Miller, *Science*, 1988, **240**, 440; (*b*) I. R. Gould and S. Farid, *Acc. Chem. Res.*, 1996, **29**, 522; (*c*) G. McLendon, *Acc. Chem. Res.*, 1988, **21**, 160; (*d*) J. R. Winkler and H. B. Gray, *Chem. Rev.*, 1992, **92**, 369; (*e*) G. McLendon and R. Hake, *Chem. Rev.*, 1992, **92**, 481.
11 (*a*) N. Mataga, T. Asahi, Y. Kanda and T. Okada, *Chem. Phys.*, 1988, **127**, 249; (*b*) N. Mataga and H. Miyasaka, in *Electron Transfer from Isolated Molecules to Biomolecules Part 2*, ed. J. Jortner and M. Bixon, Wiley, New York, 1999, p. 431.
12 (*a*) M. R. Wasielewski, *Chem. Rev.*, 1992, **92**, 435; (*b*) H. Kurreck and M. Huber, *Angew. Chem. Int. Ed. Engl.*, 1995, **34**, 849; (*c*) D. Gust and T. A. Moore, in *The Porphyrin Handbook*, ed. K. M. Kadish, K. M. Smith and R. Guilard, Academic Press, San Diego, CA, 2000, vol. 8, pp. 153–190; (*d*) D. Gust, T. A. Moore and A. L. Moore, *Acc. Chem. Res.*, 2001, **34**, 40.
13 (*a*) A. Harriman and J.-P. Sauvage, *Chem. Soc. Rev.*, 1996, **26**, 41; (*b*) M.-J. Blanco, M. C. Jiménez, J.-C. Chambron, V. Heitz, M. Linke and J.-P. Sauvage, *Chem. Soc. Rev.*, 1999, **28**, 293; (*c*) V. Balzani, A. Juris, M. Venturi, S. Campagna and S. Serroni, *Chem. Rev.*, 1996, **96**, 759.
14 (*a*) M. N. Paddon-Row, *Acc. Chem. Res.*, 1994, **27**, 18; (*b*) J. W. Verhoeven, in *Electron Transfer-From Isolated Molecules to Biomolecules*, ed. J. Jortner and M. Bixon, John Wiley & Sons, New York, 1999, Part one, pp. 603–644; (*c*) A. Osuka, N. Mataga and T. Okada, *Pure Appl. Chem.*, 1997, **69**, 797; (*d*) L. Sun, L. Hammarström, B. Åkermark and S. Styring, *Chem. Soc. Rev.*, 2001, **30**, 36.
15 (*a*) H. Imahori and Y. Sakata, *Adv. Mater.*, 1997, **9**, 537; (*b*) D. M. Guldi and M. Prato, *Acc. Chem. Res.*, 2000, **33**, 695; (*c*) S. Fukuzumi and H. Imahori, in *Electron Transfer in Chemistry*, ed. V. Balzani, Wiley-VCH, Weinheim, 2001, vol. 2, pp. 270–337; (*d*) S. Fukuzumi and D. M. Guldi, in *Electron Transfer in Chemistry*, ed. V. Balzani, Wiley-VCH, Weinheim, 2001, vol. 2, pp. 927–975.
16 L. Eberson, *Electron Transfer Reactions in Organic Chemistry; Reactivity and Structure*, Springler, Heidelberg, 1987, vol. 25.
17 W. Kaim and B. Schwederski, *Bioinorganic Chemistry: Inorganic Elements in the Chemistry of Life*, Wiley, Chichester, 1994.
18 R. Rathore and J. K. Kochi, *Adv. Phys. Org. Chem.*, 2000, **35**, 193.
19 (*a*) M. Patz and S. Fukuzumi, *J. Phys. Org. Chem.*, 1997, **10**, 129; (*b*) S. Fukuzumi, *Bull. Chem. Soc. Jpn.*, 1997, **70**, 1; (*c*) S. Fukuzumi and S. Itoh, in *Advances in Photochemistry*, ed. D. C. Neckers, D. H. Volman and G. von Bünau, Wiley, New York, 1998, vol. 25, pp. 107–172.
20 S. Fukuzumi, in *Advances in Electron Transfer Chemistry*, ed. P. S. Mariano, JAI press, Greenwich, CT, 1992, vol. 2, pp. 67–175.
21 S. Fukuzumi, in *Electron Transfer in Chemistry*, ed. V. Balzani, Wiley-VCH, Weinheim, 2001, vol. 4, pp. 3–67.
22 S. Fukuzumi, in *The Porphyrin Handbook*, ed. K. M. Kadish, K. M. Smith and R. Guilard, Academic Press, San Diego, 2000, vol. 8, pp. 115–151.
23 S. Fukuzumi, Y. Endo and H. Imahori, *J. Am. Chem. Soc.*, 2002, **124**, 10974.
24 S. Fukuzumi, K. Ohkubo, T. Suenobu, K. Kato, M. Fujitsuka and O. Ito, *J. Am. Chem. Soc.*, 2001, **123**, 8459.
25 H. P. Fritz, H. Gebauer, P. Friedrich, P. Ecker, R. Artes and U. Schubert, *Z. Naturforsch, B*, 1978, **33**, 498.
26 (*a*) R. Ratore, A. S. Kumar, S. V. Lindeman and J. K. Kochi, *J. Org. Chem.*, 1998, **63**, 5847; (*b*) J. K. Kochi, R. Rathore and P. L. Maguéres, *J. Org. Chem.*, 2000, **65**, 6826.
27 S. V. Lindeman, S. V. Rosokha, D. L. Sun and J. K. Kochi, *J. Am. Chem. Soc.*, 2002, **124**, 843.
28 R. C. Haddon, L. E. Brus and K. Raghavachari, *Chem. Phys. Lett.*, 1986, **125**, 459.
29 L. Echegoyen, F. Diederich and L. E. Echegoyen, in *Fullerenes: Chemistry, Physics, and Technology*, ed. K. M. Kadish and R. S. Ruoff, Wiley, New York, 2000, p. 1.
30 S. Fukuzumi, I. Nakanishi, T. Suenobu and K. M. Kadish, *J. Am. Chem. Soc.*, 1999, **121**, 3468.
31 D. M. Guldi and S. Fukuzumi, in *Fullerenes: From Synthesis to Optoelectronic Properties*, Kluwer Academic Publishers, Dordrecht, 2002, pp. 237–265.
32 S. Fukuzumi, K. Ohkubo, H. Imahori and D. M. Guldi, *Chem.–Eur. J.*, 2003, **9**, in press.
33 (*a*) *The Photosynthetic Reaction Center*, ed. J. Deisenhofer and J. R. Norris, Academic Press, San Diego, 1993; (*b*) *Anoxygenic Photosynthetic Bacteria*, ed. R. E. Blankenship, M. T. Madigan and C. E. Bauer, Kluwer Academic Publishing, Dordrecht, 1995.
34 C. C. Moser, C. C. Page and P. L. Dutton, in *Electron Transfer in Chemistry*, ed. V. Balzani, Wiley-VCH, Weinheim, 2001, vol. 3, pp. 24–38.
35 S. Fukuzumi, K. Ohkubo, H. Imahori, J. Shao, Z. Ou, G. Zheng, Y. Chen, R. K. Pandey, M. Fujitsuka, O. Ito and K. M. Kadish, *J. Am. Chem. Soc.*, 2001, **123**, 10676.
36 S. Fukuzumi, K. Ohkubo, Y. Chen, R. K. Pandey, R. Zhan, J. Shao and K. M. Kadish, *J. Phys. Chem. A*, 2002, **106**, 5105.
37 H. Imahori, K. Tamaki, D. M. Guldi, C. Luo, M. Fujitsuka, O. Ito, Y. Sakata and S. Fukuzumi, *J. Am. Chem. Soc.*, 2001, **123**, 2607.
38 H. Imahori, D. M. Guldi, K. Tamaki, Y. Yoshida, C. Luo, Y. Sakata and S. Fukuzumi, *J. Am. Chem. Soc.*, 2001, **123**, 6617.
39 A. Ghosh, *J. Phys. Chem., B*, 1997, **101**, 3290.

40 A. Helms, D. Heiler and G. McLendon, *J. Am. Chem. Soc.*, 1992, **114**, 6227.
41 (*a*) M. Borja and P. K. Dutta, *Nature*, 1993, **362**, 43; (*b*) P. K. Dutta and W. Turbeville, *J. Phys. Chem.*, 1992, **96**, 9410; (*c*) M. Ledney and P. K. Dutta, *J. Am. Chem. Soc.*, 1995, **117**, 7687.
42 S. Fukuzumi, Y. Yoshida, T. Urano, T. Suenobu and H. Imahori, *J. Am. Chem. Soc.*, 2001, **123**, 11331.
43 D. T. Sawyer and J. S. Valentine, *Acc. Chem. Res.*, 1981, **14**, 393.
44 S. Fukuzumi, M. Patz, T. Suenobu, Y. Kuwahara and S. Itoh, *J. Am. Chem. Soc.*, 1999, **121**, 1605.
45 S. Fukuzumi and K. Ohkubo, *Eur.–J. Chem.*, 2000, **6**, 4532.
46 K. Ohkubo, T. Suenobu, H. Imahori, A. Orita, J. Otera and S. Fukuzumi, *Chem. Lett.*, 2001, 978.
47 S. Fukuzumi, N. Satoh, T. Okamoto, K. Yasui, T. Suenobu, Y. Seko, M. Fujitsuka and O. Ito, *J. Am. Chem. Soc.*, 2001, **123**, 7756.
48 S. Fukuzumi and K. Ohkubo, *J. Am. Chem. Soc.*, 2002, **124**, 10270.
49 S. Fukuzumi, H. Imahori, H. Yamada, M. E. El-Khouly, M. Fujitsuka, O. Ito and D. M. Guldi, *J. Am. Chem. Soc.*, 2001, **123**, 2571.
50 I. Fridovich, *Annu. Rev. Biochem.*, 1995, **64**, 97.
51 H. Ohtsu, Y. Shimazaki, A. Odani, O. Yamauchi, S. Itoh and S. Fukuzumi, *J. Am. Chem. Soc.*, 2000, **122**, 5733.
52 H. Ohtsu and S. Fukuzumi, *Angew. Chem. Int. Ed.*, 2000, **39**, 4537.
53 H. Ohtsu and S. Fukuzumi, *Chem.–Eur. J.*, 2001, **7**, 4947.
54 S. Fukuzumi, K. Okamoto and H. Imahori, *Angew. Chem. Int. Ed.*, 2002, **41**, 620.
55 S. Fukuzumi, K. Okamoto, Y. Yoshida, H. Imahori, Y. Araki and O. Ito, *J. Am. Chem. Soc.*, 2003, **125**, 1007.
56 S. Fukuzumi, Y. Yoshida, K. Okamoto, H. Imahori, Y. Araki and O. Ito, *J. Am. Chem. Soc.*, 2002, **124**, 6794.
57 S. Fukuzumi, S. Koumitsu, K. Hironaka and T. Tanaka, *J. Am. Chem. Soc.*, 1987, **109**, 305.
58 S. Fukuzumi, Y. Fuji and T. Suenobu, *J. Am. Chem. Soc.*, 2001, **123**, 10191.
59 S. Fukuzumi, H. Mori, H. Imahori, T. Suenobu, Y. Araki, O. Ito and K. M. Kadish, *J. Am. Chem. Soc.*, 2001, **123**, 12458.
60 S. Fukuzumi, O. Inada, N. Satoh, T. Suenobu and H. Imahori, *J. Am. Chem. Soc.*, 2002, **124**, 9181.
61 S. Fukuzumi and T. Okamoto, *J. Am. Chem. Soc.*, 1993, **115**, 11600.
62 S. Fukuzumi, K. Ohkubo and T. Okamoto, *J. Am. Chem. Soc.*, 2002, **124**, 14147.
63 S. Fukuzumi, J. Yuasa and T. Suenobu, *J. Am. Chem. Soc.*, 2002, **124**, 12566.